RESEARCH ARTICLE

Molecular Docking and Simulation Analysis of Cyclopeptides as Anti-cancer Agents

Abhishek Tiwari[1,*], Varsha Tiwari[1], Suresh Kumar[2], Manish Kumar[3], Renu Saharan[3], Navneet Varma[1], Biswa Mohan Sahoo[4], Deepak Kaushik[5] and Rajeev Kumar Sharma[6]

[1]*Pharmacy Academy, IFTM University, Lodhipur-Rajput, Moradabad-244102, India;* [2]*Bharat Institute of Pharmacy, Pehladpur, Babain, Kurukshetra, Haryana-136156, India;* [3]*M M College of Pharmacy, Maharishi Markandeshwar (Deemed to be University), Mullana, Ambala-133207, Haryana, India;* [4]*Roland Institute of Pharmaceutical Sciences, Berhampur-760010, Odisha, India;* [5]*Department of Pharmaceutical Sciences, M. D. University, Rohtak 124001, Haryana, India;* [6]*Department of Pharmaceutical Chemistry, Faculty of Pharmacy, DIT University, Mussorie Diversion Road, Village Makkawala, Dehradun, Uttarakhand 248009, India*

Abstract: ***Background*:** Cancer is a leading cause of death for people worldwide, in addition to the rise in mortality rates attributed to the Covid epidemic. This allows scientists to do additional research. Here, we have selected Integerrimide A, cordy heptapeptide, and Oligotetrapeptide as the three cyclic proteins that will be further studied and investigated in this context.

***Methods*:** Docking research was carried out using the protein complexes 1FKB and 1YET, downloaded from the PDB database and used in the docking investigations. Cyclopeptides have been reported to bind molecularly to human HSP90 (Heat shock protein) and FK506. It was possible to locate HSP90 in Protein Data Banks 1YET and 1FKB. HSP90 was retrieved from Protein Data Bank 1YET and 1FKB. Based on these findings, it is possible that the anticancer effects of Int A, Cordy, and Oligo substances could be due to their ability to inhibit the mTOR rapamycin binding domain and the HSP90 Geldanamycin binding domain via the mTOR and mTOR chaperone pathways. During the calculation, there were three stages: system development, energy reduction, and molecular dynamics (also known as molecular dynamics). Each of the three compounds demonstrated a binding affinity for mTOR's Rapamycin binding site that ranged from -6.80 to -9.20 Kcal/mol (FKB12).

***Results*:** An inhibition constant Ki of 181.05 nM characterized Cordy A with the highest binding affinity (-9.20 Kcal/mol). Among the three tested compounds, Cordy A was selected for MD simulation. HCT116 and B16F10 cell lines were used to test each compound's anticancer efficacy. Doxorubicin was used as a standard drug. The cytotoxic activity of substances Int A, Cordy A, and Oligo on HCT116 cell lines was found to be 77.65 µM, 145.36 µM, and 175.54 µM when compared to Doxorubicin 48.62 µM, similarly utilizing B16F10 cell lines was found to be 68.63 µM, 127.63 µM, and 139.11 µM to Doxorubicin 45.25 µM.

***Conclusion*:** Compound Cordy A was more effective than any other cyclic peptides tested in this investigation.

ARTICLE HISTORY

Received: July 22, 2022
Revised: November 20, 2022
Accepted: December 16, 2022

DOI:
10.2174/1574885518666230222113033

Keywords: Integerrimide A, cordyheptapeptide A, oligotetrapeptide, Hsp90, HCT116, B16F10.

1. INTRODUCTION

Mortality from cancer is second only to heart disease as a main cause of death globally [1, 2]. In 2002, 7.1 million people died from cancer. By 2030, that number is expected to rise to 11.5 million [1]. Men are more likely to get colorectal and lung cancer, whereas women are more likely to develop breast, colorectal, and cervical cancers [3]. Many cancer therapies are available, including chemotherapy, radiation therapy, and surgery [4]. Conventional cancer treatment methods have a variety of drawbacks, and one of these is the potential for side effects and toxicity [5]. New effective medications for preventing and treating this illness with the fewest side effects are needed because standard chemotherapeutic tactics have failed, and plants can be an important source of these promising compounds [6].

Regarding treating various illnesses, including cancer, plants have played an important role. All modern medications are produced directly or indirectly from higher plants, which shows the enormous potential of the plants that have been utilized for years [7]. In addition, plant-based anticancer medicines make up roughly 60% of all anticancer medications [8].

*Address correspondence to this author at the Pharmacy Academy, IFTM University, Lodhipur-Rajput, Moradabad-244102, India;
Tel: +91-6398884097; E-mail: abhishekt1983@gmail.com

1574-8855/XX $65.00+.00

Cyclic peptides are polypeptide chains with a cyclic ring structure. The ring structure is created by joining one end of the peptide to the other with an amide bond or another chemically stable bond such as lactone, ether, thioether, or disulfide. C-to-N (or head-to-tail). The formation of amide bonds between the amino and carboxyl termini occurs during cyclization, and this process is employed to synthesize a significant variety of physiologically active cyclic peptides. While peptides have historically been thought to be inefficient therapeutic agents, they have certain benefits. The following parts describe the limitations of the peptides; the ones highlight the strengths. To begin, oral absorption of peptide medicine is weak.

Because the gastrointestinal system absorbs peptides poorly, injection is the most common delivery method. Second, even after effective absorption, proteolytic enzymes rapidly destroy peptides. Third, unlike certain tiny compounds, peptides normally do not cross the cell membrane. If the target of a peptide medicine resides in the cytoplasm, the peptide may never reach the target. Despite these constraints, peptides may be preferred to tiny synthesized compounds for the reasons listed below. Peptides are less hazardous than minutely synthesized compounds and would be dangerous if not synthesized [9]. Because of their precise contact with their targets, peptides can work selectively with them [10]. Cyclic peptide stiffness reduces the entropy term of the Gibbs free energy, allowing for improved binding to target molecules or receptor selectivity. The cyclic structure is also resistant to exopeptidase hydrolysis due to the lack of amino and carboxyl termini [11]. The cyclic peptides Integerrimide A (1) [Int A (1)], Cordyheptapeptide A (2) [Cordy A (2)], and Oligotetrapeptide (3) [Oligo (3)] were taken for the study. Doxorubicin (4) was used as a reference compound (Fig. **1**).

The heat shock protein 90 (HSP90) is a chaperone protein responsible for the maturation and function of a range of critical client proteins engaged in cellular activities [12-14]. This protein is overexpressed in tumour cells, causing uncontrolled cell growth. The capacity of HSP90 N-terminal domain to bind and hydrolyze ATP is critical to its activity [12, 15, 16]. An intrinsic ATPase activity is essential for functioning a functional chaperone cycle, which results in the stabilization of client proteins. [12, 13, 17], The second target considered is 1FKB, which is the target of FK506, a new immunosuppressive drug [18]. Using molecular docking, the authors investigated the binding capacity of cyclopeptides to human HSP90 and FK506. The Protein Data Bank (PDB codes: 1YET&1FKB) was used to get HSP90.

2. MATERIALS AND METHODS

2.1. Hardware and Software

The molecular docking study of the synthesized peptides was performed on Windows 10 (64-bit) operating system with 4 GB RAM and a 2.50 GHz Intel(R) Core (TM) i5-7200U processor. Autodock Tools 4.2.6 and MGL Tools version 1.5.7 were utilized to carry out molecular docking [19], which are made available for free by the Scripps Research Institute at https://autodock.scripps.edu/. The other software requirements have been specified, along with the protocols used.

2.2. Selection of Target Proteins

Rapamycin-FKB12 subunit of mTOR (PDB ID: 1FKB) and Geldanamycin-human Hsp90 Chaperone (PDB ID: 1YET) complexes were chosen as target proteins for performing docking studies. The overexpression of mTOR and Hsp90 in melanoma and colon cancer [20-22] and the presence of macrocyclic inhibitors, *i.e.*, Rapamycin in 1FKB [22] and Geldanamycin in 1YET [23] crystal structures justify the rationale for the choice of these proteins. It was anticipated that the synthesized macrocyclic ligands would bind optimally at the binding sites occupied by Rapamycin and Geldanamycin in proteins 1FKB and 1YET, respectively. The results can also be correlated with *in vitro* results for anticancer potential against melanoma (B16F10) and colon cancer (HCT-116) cell lines.

2.3. Protein and Ligand Processing for Docking Protein Preparation

Protein Data Bank files of Rapamycin-FKB12 subunit of mTOR (PDB ID: 1FKB) and Geldanamycin-human Hsp90 (PDB ID: 1YET) complexes were downloaded from the RCSB database. Protein preparation was carried out us-

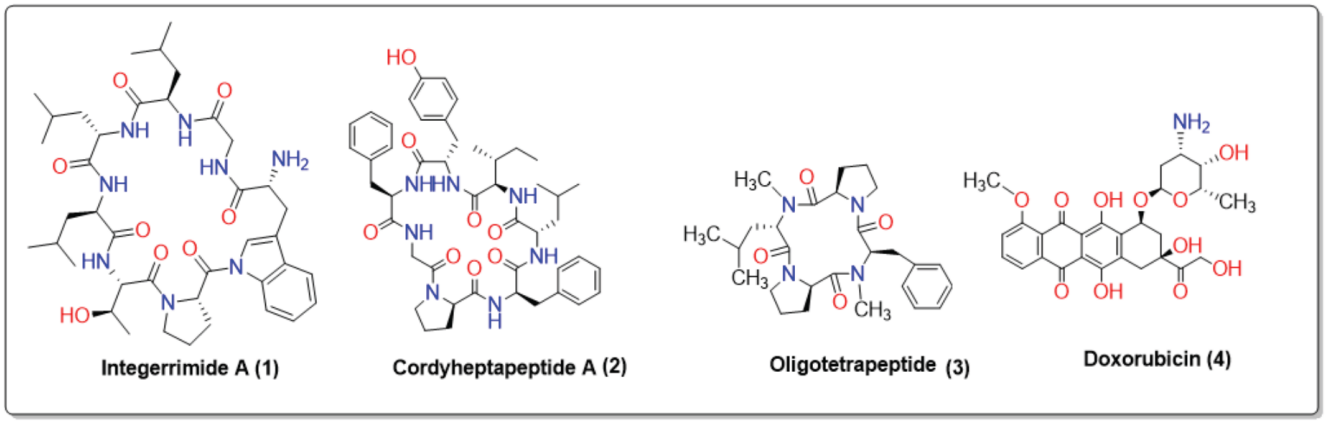

Fig. (1). Cyclic peptides used for the docking and doxorubicin as standard drug.

ing the Autodock Wizard by deleting attached water molecules, bound heteroatoms/ligand, adding polar hydrogens, kollman charges, spreading charge equally over all atoms and checking for missing atoms on residues. The PDB files were then converted to the PDBQT format for executing the next step.

2.4. Ligand Preparation

Ligand structures were drawn on Chem Bio Draw Ultra 14.0, minimized using MM2 forcefield in the Chem3DPro 14.0 software, and saved as PDB files. The ligands were then prepared using Autodock tools, where nonpolar hydrogens were merged, Gasteiger charges added, and torsions were set as specified one by one for each ligand. The ligand files were then saved in the PDBQT format.

2.5. Grid Generation

For carrying out docking between prepared receptors and ligands, the grid was generated by taking the center of the attached ligand. The grid dimensions were specified as 3.773 x 12.503 x 13.752 Å3 with spacing 0.375, keeping several points as 40 in X, Y, and Z direction for PDB ID: 1FKB and 40.85 x -46.782 x 65.663 Å3 with spacing 0.375, keeping the number of points as 40 in X, Y, Z direction for PDB ID: 1YET. Map types were set for each ligand individually.

2.6. Docking and Visualization of Results

After the grid generation, docking was carried out using the Lamarckian Genetic algorithm with default genetic algorithm parameters, and the results were saved as docking log files for individual ligands. The conformations for each ligand were analyzed, and the best conformations were taken, keeping the binding energy as the criteria. The 3D and 2D interaction diagrams were created using Discovery Studio Visualizer.

2.7. Molecular Dynamics Simulation (MDS) Analysis

The Schrödinger Desmond tool was used to simulate ligand-protein complexes [24]. Based on the number of docking score parameters, the top two compounds from all screened compounds were chosen for MD simulations. System builder, energy minimization, and molecular dynamics were all used in the simulation. A solvated system was developed using SPC as the solvent model and POPC as the membrane with an orthorhombic box form. A buffer was chosen for box size computation at a distance of 10.0 Å. The physiological state of the simulation box was achieved by neutralizing the charge and adjusting the salt content to 0.15 M of Na^+ and Cl^- ions. The volume of the simulation box is minimized by aligning the major axes of the solute along the box vectors or the diagonal. The solvated system contains proteins, protein complexes, protein-ligand complexes, proteins submerged in a membrane bilayer, and other solutes. A maximum of 2000 iterations reduced the energy of the ligand-protein combination to remove steric conflicts. The MD tab's work area was filled with the pre-processed ligand-protein combination, and the NPT ensemble was set to 300.0 K temperature and 1.01325 bar pressure. Fifty ns simulations were run after the model system was relaxed, and the ligand-protein complex's trajectory was recorded at 4.8 ps. [25] To validate the complex's conformational behaviour and stability across a 50-ns simulation, researchers looked at energy, ligand-protein RMSD, RMSF, protein-ligand interactions, and ligand characteristics.

2.8. Anti-cancer Activity

All cyclic peptides were collected from the lab of the Institute of Pharmaceutical Sciences, Kurukshetra University, Kurukshetra, Haryana. The cytotoxicity of the compounds was carried out at Deshpandey Laboratories Pvt. Ltd. in Bhopal, India, by using Doxorubicin as standard, on HCT116 and B16F10 cell lines, using MTT [(3-[4,5-dimethylthiazol-2Yl]-2,5-diphenyl-tetrazolium bromide)] test. B16F10 cell lines originate from mouse skin cancer, whereas HCT116 cell lines originate from human colorectal cancer. HCT116 and B16F10 cell lines were used to test the cytotoxic activity by measuring the percentage of growth suppression. The graphical extrapolation approach was used to calculate the CTC50 values (cytotoxic concentration at 50% cell death following drug exposure). For the test, control, and routine medicine, 120-7.5 g/mL was used [26]. Colorimetric measurements of MTT conversion into formazan crystals by living cells, which evaluates mitochondrial activity, constitute the basis of this method's methodological concept. After being transformed into a dark purple formazan complex that is insoluble inside the cells, MTT is expelled from the body. A spectrophotometer was used to measure the formazan reagent in the cells after they were mixed with isopropanol. CO_2 incubator with phosphate-buffered saline (PBS), 96-well plate with a flat bottom MTT reagent, acidic pH isopropanol, and a 96-well plate. For cytotoxic analysis, 5000-10000 cells of the HCT116 and B16F10 cell lines were placed in a 96-well tissue culture plate with 100 l of RPMI-1640 culture media in a tissue culture dish with a flat bottom. Before testing cyclic peptides, the aforementioned combination was allowed to rest overnight for cell adhesion. MTT reagent (5 mg/ml) was then applied to each well and incubated at 37°C for 4 hours to allow the MTT cleavage to give colour to the samples. In each well of the aforementioned mixture, 0.1 ml of acidic isopropanol was carefully added using a multichannel pipettor. The yellow colour produced by the HCl reaction with phenol red growth media makes MTT-formazan measurement straightforward. Formazan was mixed with isopropanol to produce a blue solution. A plate reader was used to measure the optical density of the test medicine at 570 nm and the reference medication at 630 nm (Fig. **2**). The following formula was used to figure out the percentage of growth inhibition.

3. RESULTS AND DISCUSSION

3.1. PDB ID: 1FKB

The docking results suggest that all compounds interacted with the Rapamycin binding site of mTOR (FKB12) and displayed binding affinities between -6.80 to -9.20 Kcal/mol. All compounds, except In A, had better binding affinity than the reference compound Doxorubicin. The interactions of all compounds have been presented in Table **1**

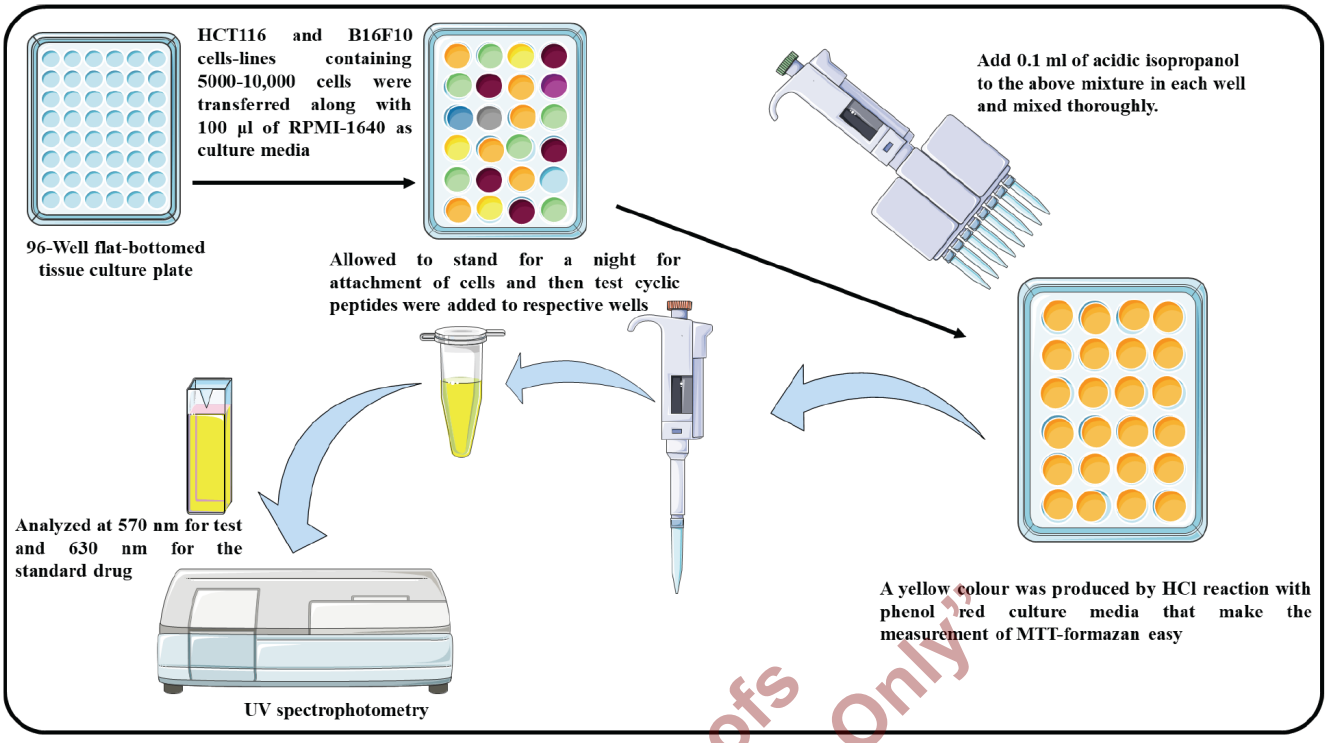

Fig. (2). Procedure of anticancer activity. (*A higher resolution / colour version of this figure is available in the electronic copy of the article*).

Table 1. Docking results (PDB ID: 1FKB).

S. No.	Compound	Binding Energy (Kcal/mol)	Inhibition Constant (Ki)	Hydrogen Bonding Interactions (Conventional)	Receptor Ligand Interactions
a)	**1**	-6.80	10.33 µM	-	Phe46;Glu54;Val55; Tyr82;His87
b)	**2**	-7.16	5.69µM	Tyr26;Asp37; Glu54	Phe46;Val55
c)	**3**	-8.40	695.02 nM	-	Tyr26;Ile91; Asp37;Phe46;Val55;Ile56; Trp59;Glu54;Tyr82;Phe36;Phe99;His 87
d)	**4** (Reference)	-7.02	7.15 µM	Ile56;Tyr82	Asp37; Trp59;His87;Ile90

and Figs. (**3-6**). Oligoes displayed the best binding affinity of -8.40 Kcal/mol, inhibition constant Ki of 695.02 nM, interacted with Phe46 *via* π-π, T stacking Val55; Ile56; Ile91 *via* alkyl interactions and Phe36; Trp59; Tyr82; His87; Phe99 *via* π-alkyl interactions (Fig. **6**).

3.2. Proposed Mechanism

mTOR coordinates cell proliferation, apoptosis, and autophagy, among other things, in the body through a variety of signaling pathways. The mTOR signaling pathway has also been related to cancer, tumors, insulin resistance, osteoporosis, arthritis, and other diseases, according to research. This pathway activates tumors and controls gene transcription and translation processes such as cell proliferation and immune cell variation. It also plays an important role in tumor and cancer development. Recently, mTOR inhibitors have been demonstrated to be particularly successful in cancer therapy in clinical trials. Cyclopeptides have also shown a strong affinity to this receptor, suggesting they might be used as mTOR inhibitors [27].

3.3. PDB ID: 1YET

The docking results suggest that all compounds interacted with the Geldanamycin binding site of Hsp90 and displayed binding affinities between -5.17 to -9.52 Kcal/mol. All compounds, except In A, had better binding affinity than

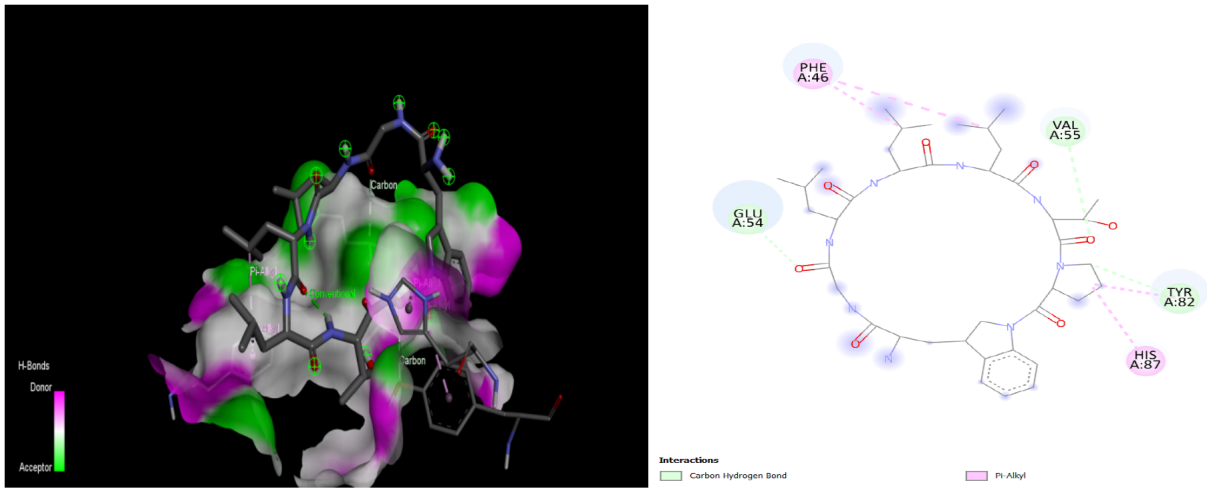

Fig. (3). 3D and 2D binding conformation of Integerrimide-A at rapamycin binding site of mTOR (PDB ID: 1FKB). (*A higher resolution / colour version of this figure is available in the electronic copy of the article*).

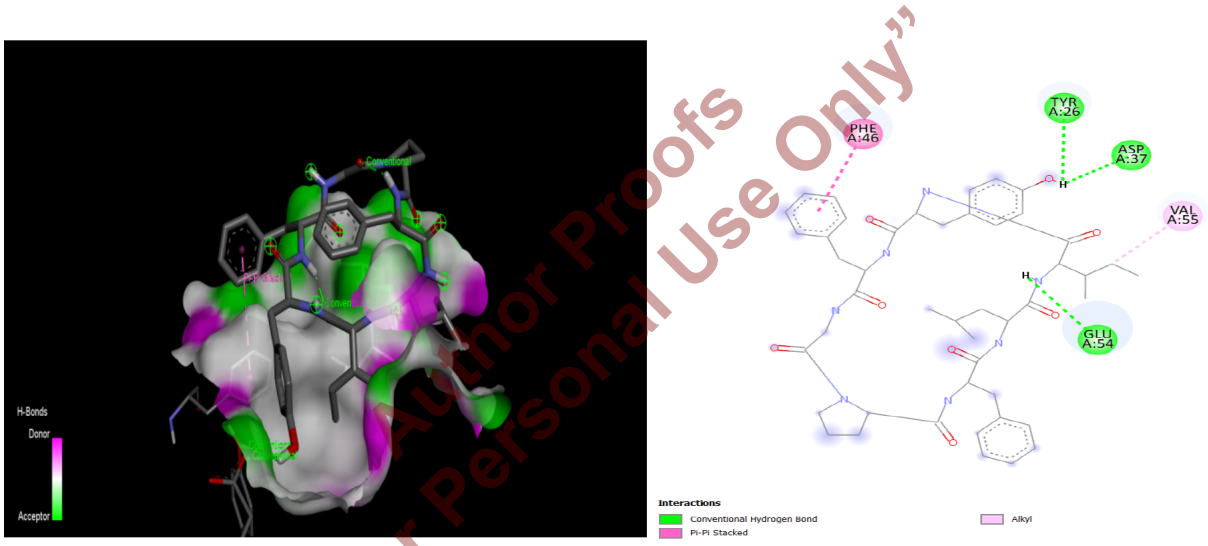

Fig. (4). 3D and 2D binding conformation of Cordy Aat Rapamycin binding site of mTOR (PDB ID: 1FKB). (*A higher resolution / colour version of this figure is available in the electronic copy of the article*).

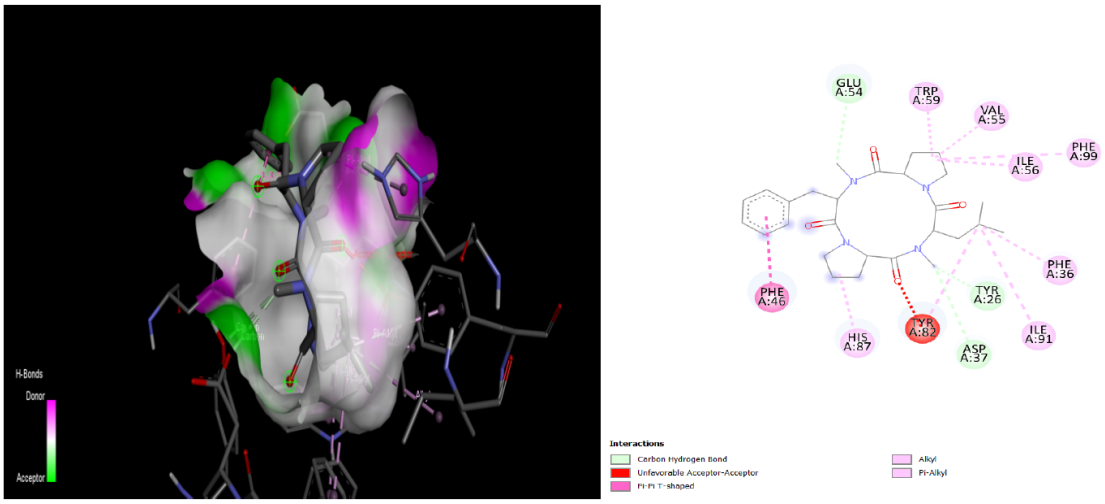

Fig. (5). 3D and 2D binding conformation of Oligoat Rapamycin binding site of mTOR (PDB ID: 1FKB). (*A higher resolution / colour version of this figure is available in the electronic copy of the article*).

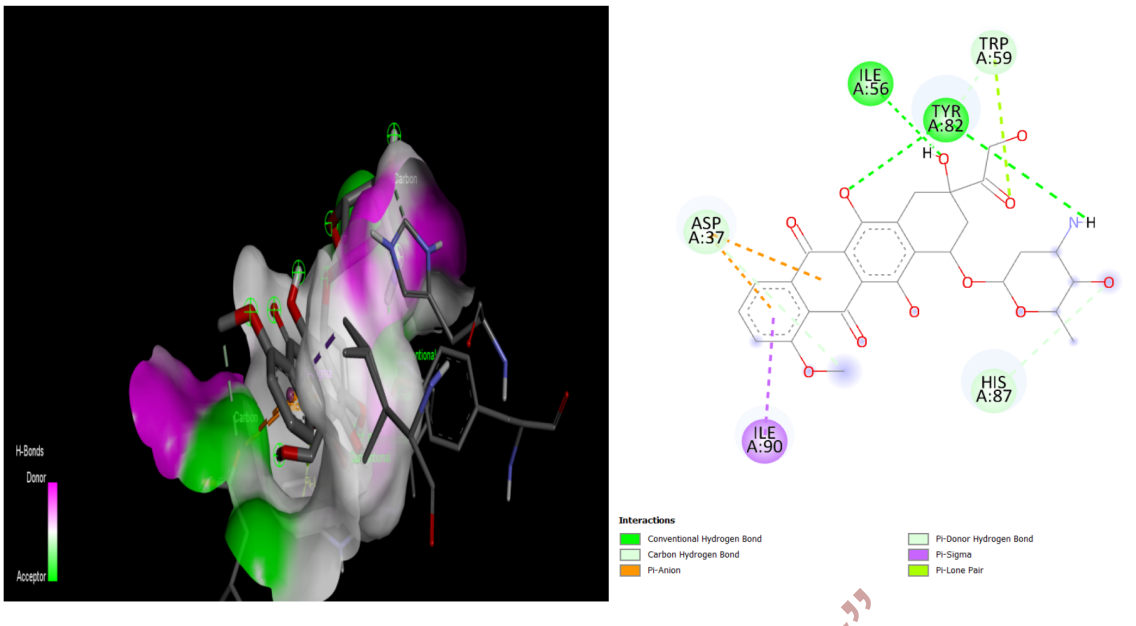

Fig. (6). 3D and 2D binding conformation of Doxorubicin (Reference) at Rapamycin binding site of mTOR (PDB ID: 1FKB). (*A higher resolution / colour version of this figure is available in the electronic copy of the article*).

Table 2. Docking results (PDB ID: 1YET).

S. No.	Compound	Binding Energy (Kcal/mol)	Inhibition Constant (Ki)	Hydrogen Bonding Interactions (Conventional)	Receptor Ligand Interactions
1.	Int A	-5.17	161.21 µM	Asp54;Lys58; Lys112	Ala55;Ile96;Phe138
2.	Cordy A	-9.52	104.30 nM	Asn51;Ser52; Lys112; Gly135;Phe138	Asp54;Ala55;Asp93;Ile96;Met98;Asp102; Tyr139
6.	Oligo	-8.37	732.57 nM	Lys58	Ala55; Ile96; Met98
7.	Doxorubicin (Reference)	-7.02	3.08 µM	Asn51;Lys58; Asn106;Lys112;Glu135;Phe138	Asp54;Ala55;Met98

the reference compound Doxorubicin. The details of the interactions of all compounds have been presented in Table **2** and (Figs. **7-10**). Cordy A displayed the best binding affinity of -9.52 Kcal/mol, inhibition constant Ki of 104.30 nM, interacting with residues Asp54; Asp93, Asp102 *via* π-anion interactions, Met98 *via* π-sulfur interaction, Ala55; Ile96; Tyr139 *via* π-alkyl interactions, Lys 112 *via* alkyl interactions and with Asn51; Ser52; Lys112; Gly135; Phe138 *via* conventional hydrogen bond interactions (Fig. **9**).

The docking results suggest that the synthesized compounds have the potential to inhibit the rapamycin binding domain of mTOR (FKB12) and the geldanamycin binding domain of Hsp90; they may exert anticancer action against melanoma and colon cancer by inhibition of mTOR and Hsp90 Chaperone.

3.4. Proposed Mechanism

Hsp90 is an ATP-dependent molecular protein that affects late-stage maturation, stability, and activation of various proteins (Hsp90 inhibitors). Hsp90 inhibitors have been connected to signal transduction and other pathways and may play a role in cancer. Hsp90 is highly expressed in normal cells and helps them maintain homeostasis, but cancer cells make use of it:

a) It promotes the expression of oncoproteins and various kinases and transcription factors that can be mutated, overexpressed, or otherwise altered in cancer.

b) To alleviate the cellular stress caused by a carcinogenic lifestyle. Hsp90 is typically overexpressed in cancer cells and is considered important for malignant conversion and development.

Hsp90-dependent pathways promote unrestricted growth, the ability to survive in low-oxygen environments, and handle nutritional deprivation, among other things. Inhibition of Hsp90 promotes activated tumor death. Hsp90 inhibitors may help vaccinations that activate the immune system work more effectively. Cyclopeptides were also shown to have a promising interaction with this protein,

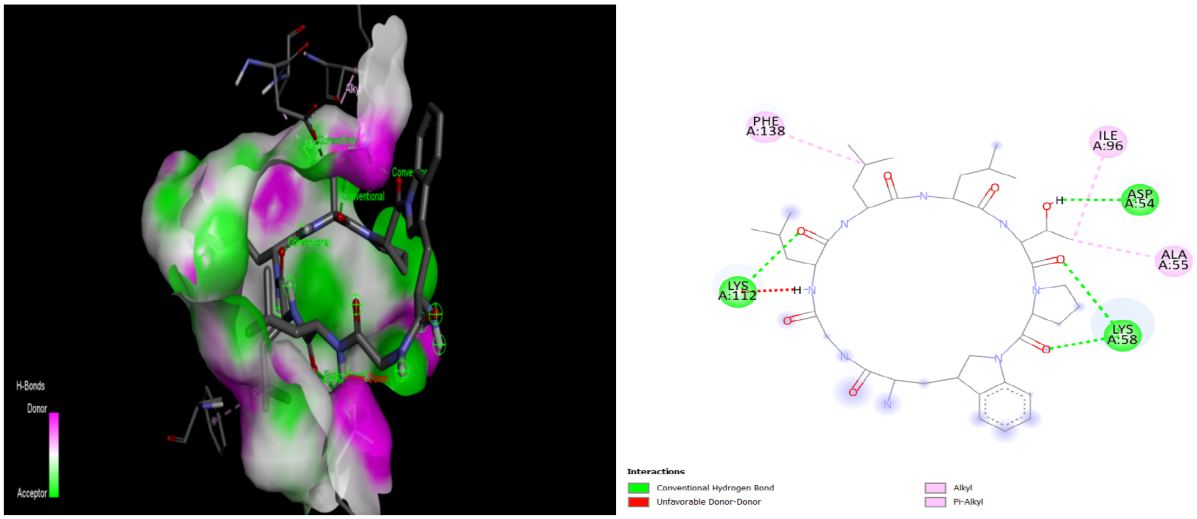

Fig. (7). 3D and 2D binding conformation of Integerrimide-A at Geldanamycin binding site of Hsp90 (PDB ID: 1YET). (*A higher resolution / colour version of this figure is available in the electronic copy of the article*).

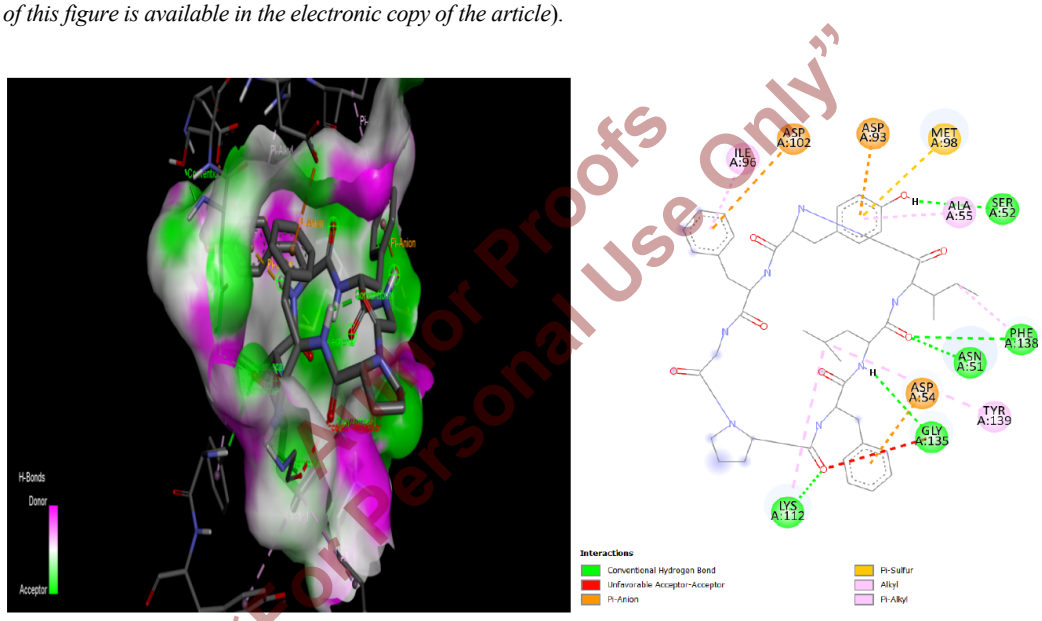

Fig. (8). 3D and 2D binding conformation of Cordy A at Geldanamycin binding site of Hsp90 (PDB ID: 1YET). (*A higher resolution / colour version of this figure is available in the electronic copy of the article*).

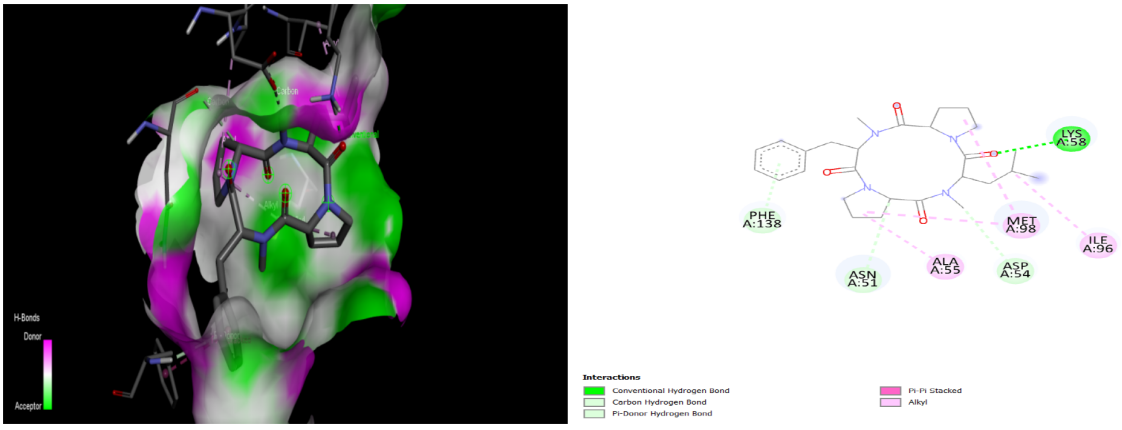

Fig. (9). 3D and 2D binding conformation of Oligoat Geldanamycin binding site of Hsp90 (PDB ID: 1YET). (*A higher resolution / colour version of this figure is available in the electronic copy of the article*).

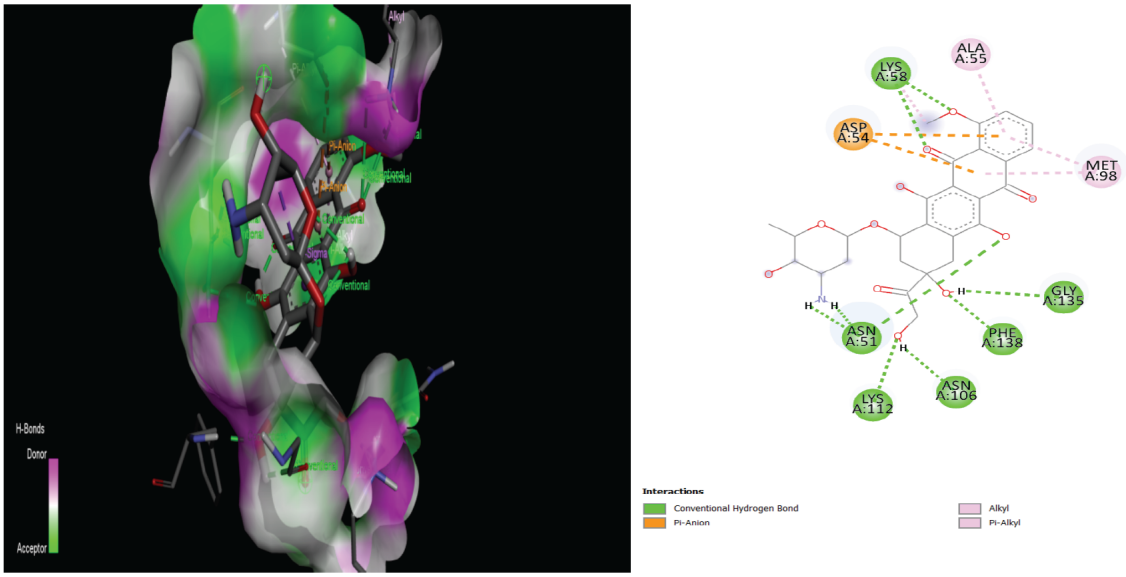

Fig. (10). 3D and 2D binding conformation of Doxorubicin (Reference) at Geldanamycin binding site of Hsp90 (PDB ID: 1YET). (*A higher resolution / colour version of this figure is available in the electronic copy of the article*).

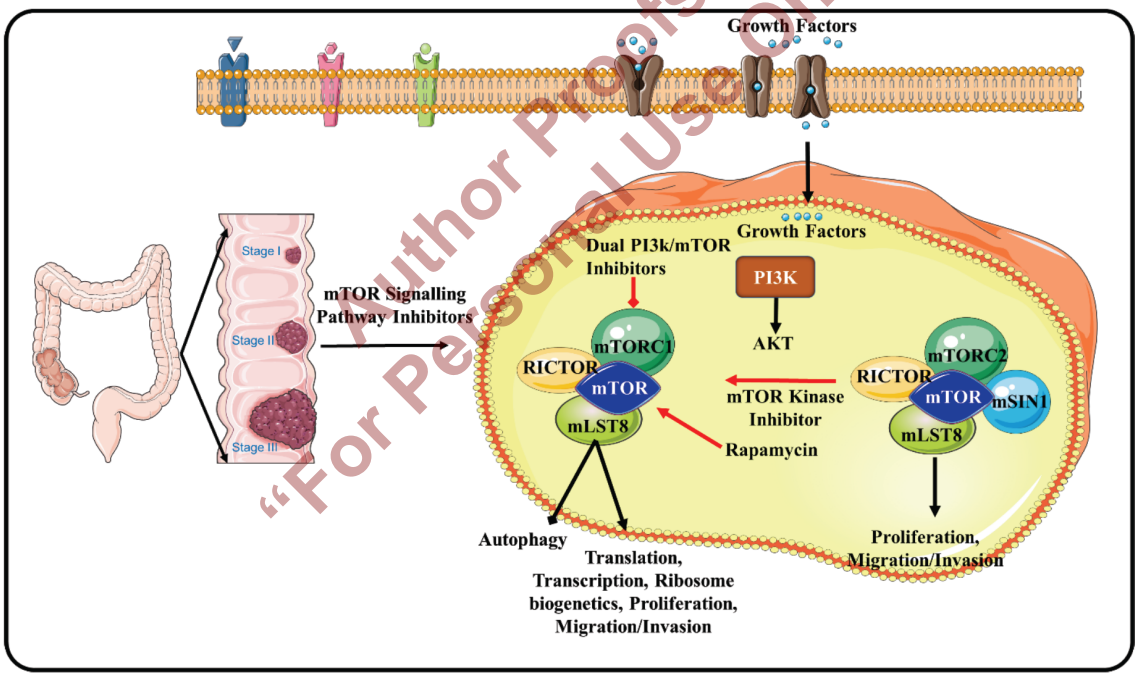

Fig. (11). Mechanism of mTOR signaling Inhibition. Drug when binds to m TOR in presence of m TOR kinase enzyme inhibits the proteins leads to activation of Autophagy, translation, transcription, Ribosome, migration, proliferation and Invasion. (*A higher resolution / colour version of this figure is available in the electronic copy of the article*).

suggesting that cyclopeptides might operate as potential inhibitors through this pathway. As a result, cyclopeptide will undoubtedly be the preferred treatment for cancer and tumors, including metastasis. Further study is required to understand these chemicals fully [28, 29] (Figs. **11**, **12**).

3.5. MD Simulation for Ligand Cordy A-1YET Complex

MD simulation at 50ns was done for top docked molecule Cordy A. MD simulations were carried out to investigate the stability of the interactions of ligand-protein docked complexes. In MD simulations, RMSD analysis of the protein backbone with respect to the original frame structure was taken up to evaluate the stability of the protein (1YET) with inhibitor (Cordy A) bound at the Geldanamycin binding site. The secondary protein structure has % Helix 24.91, % Strand 20.51, and % SSE 45.42. The RMSD values of protein and ligand were consistent at 4.5 Å and 3.8 Å correspondingly in a 35-50 ns time frame (Fig. **13**). The RMSF plots of protein (backbone) and ligand exhibited little changes below 1.6 Å and 1.5 Å correspondingly (Figs. **14** and **15**). The interactions throughout the 50 ns trajectory

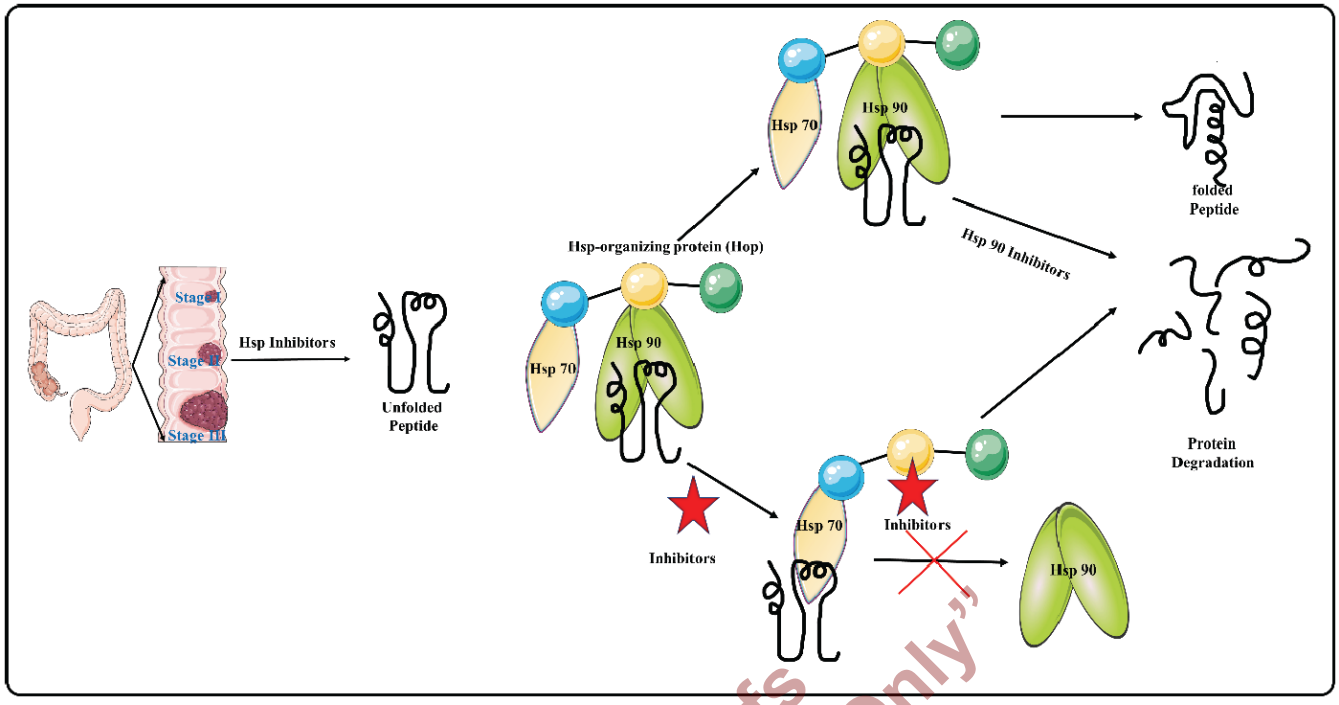

Fig. (12). Mechanism of Hsp 90 Inhibition. Hsp inhibitors when combined with Hsp protein namely Hsp 70 and 90 respectively. Inhibitors when combined to Hsp 90 part leads to protein folding. When inhibitor combined with Hsp 70 leads to denaturation of protein leads to fragmentation of protein. (*A higher resolution / colour version of this figure is available in the electronic copy of the article*).

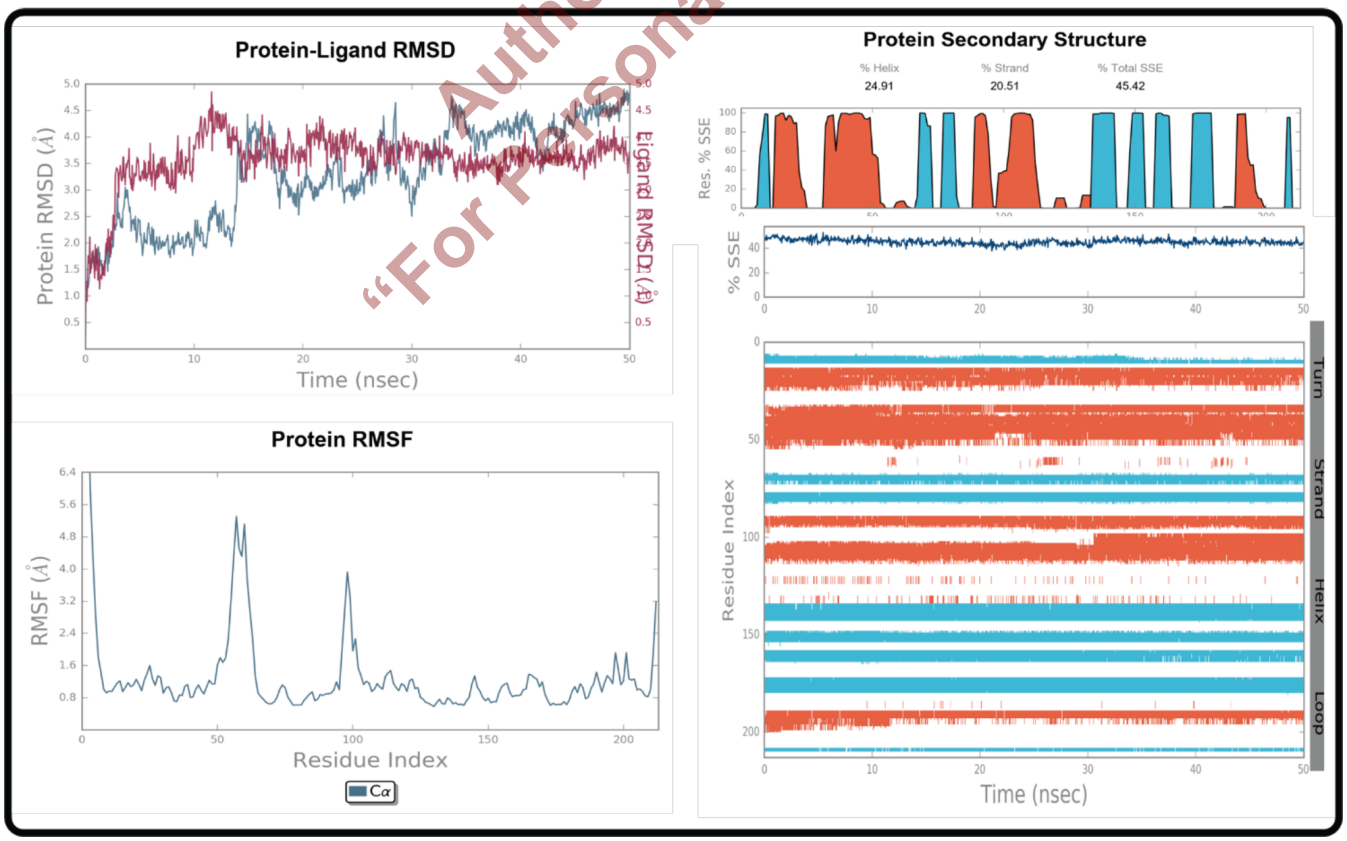

Fig. (13). Root mean square deviation (RMSD) of protein (1YET) and ligand (Cordy A) during 50 ns of MD simulation. (*A higher resolution / colour version of this figure is available in the electronic copy of the article*).

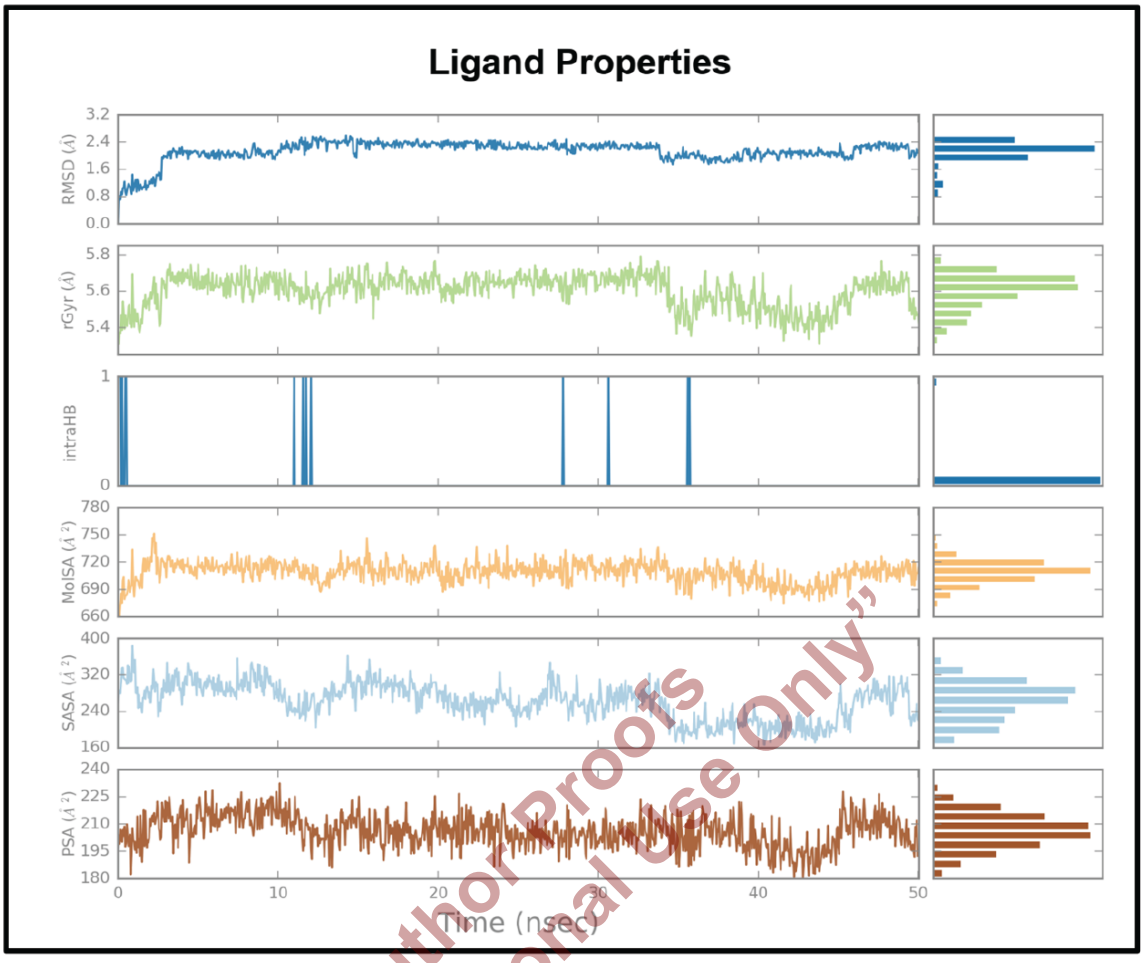

Fig. (14). Comparision of RMSD, rGyr (Å), intraHB, MolSA (Å^2), SASA (Å^2), PSA (Å^2).

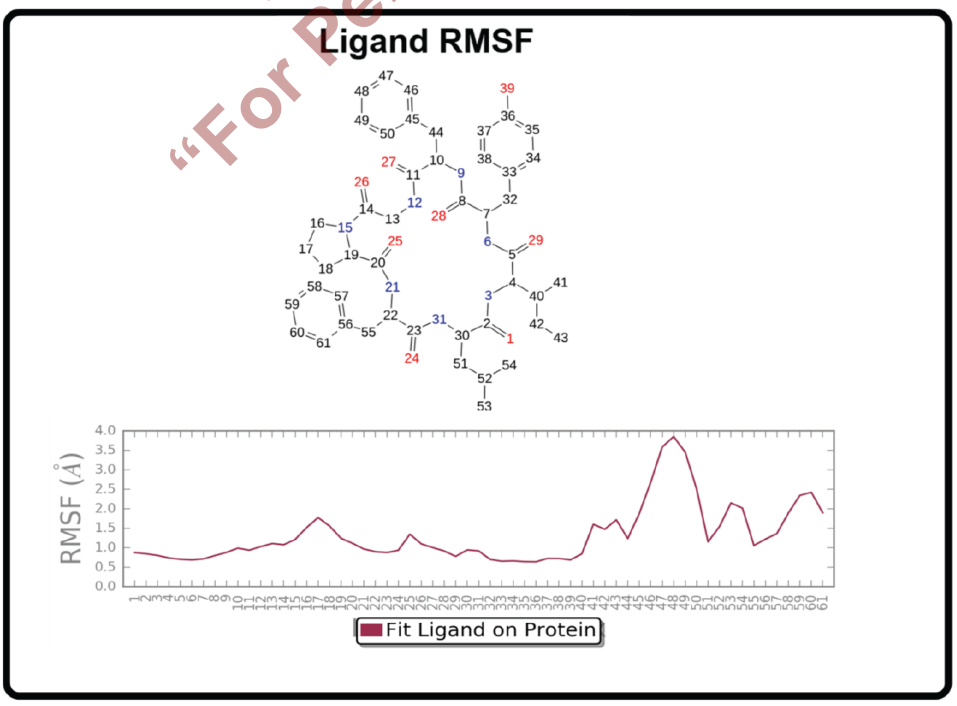

Fig. (15). Root mean square fluctuation (RMSF) plot of ligand Cordy A.

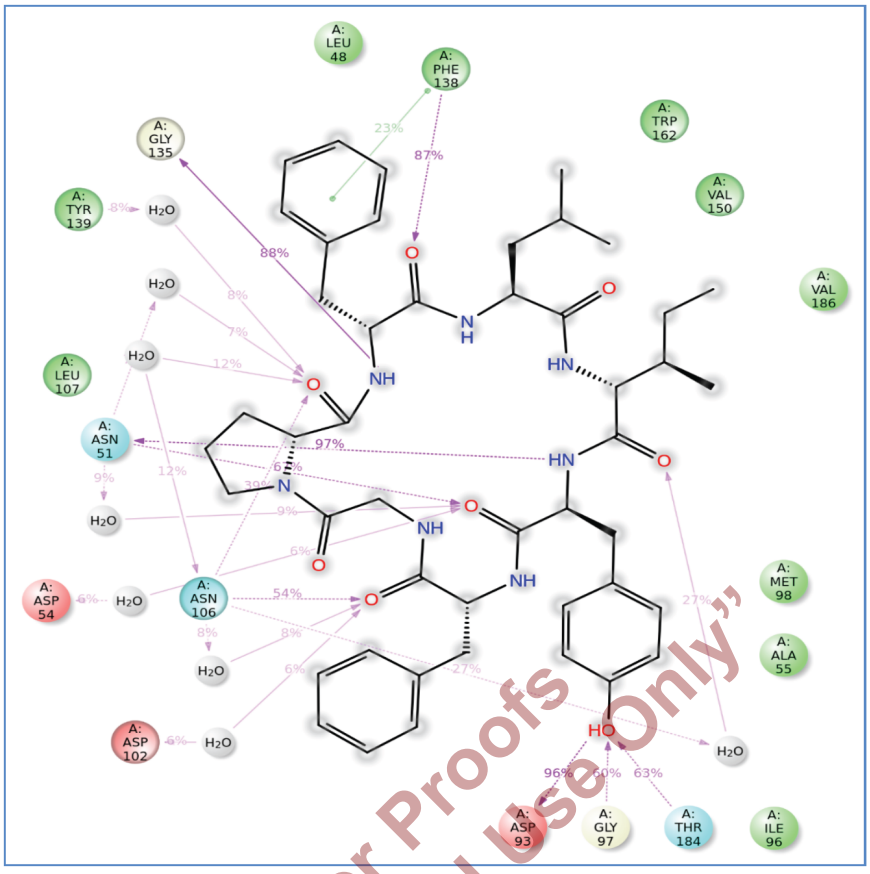

Fig. (16). Binding interactions of ligand Cordy A with 1YET during MD Simulation of 50 ns. (*A higher resolution / colour version of this figure is available in the electronic copy of the article*).

were studied, where residues Asp93, Gly97, Gly135, Phe138, and Thr184 were engaged in hydrogen bond contacts with protein, Asn51, Asp54, Asn106, Asp107 interacted through water bridges, and Phe138 showed π- π stacking interaction (Fig. **16**). The interaction fraction of various amino acid residues has been reported in Fig. (**17**).

4. BIOLOGICAL EVALUATION

Cyclic peptides are a significant family of molecules with a diverse biological profile. The cytotoxic activity of the cyclic peptides is shown in Table **3**. Fig. (**18**) shows the cytotoxic activity of cyclic peptides in the HCT116 cell line, and Fig. (**19**) shows the cytotoxic activity of cyclic peptides in the B16F10 cell line.

At a 120 g/mL concentration, cyclopeptide IG A inhibited cell proliferation by 87.5 and 72.5% against HCT116 and B16F10 cell lines, respectively. Cyclopeptide IG A demonstrated CTC50 values of 77.65 µM and 68.63 µM against HCT116 and B16F10, respectively. The % growth inhibitions at lesser dosages are 72.5 and 50 at 60 g/mL, respectively. The standard drug, Doxorubicin, inhibited growth by 100 percent with CTC50 values of 48.63 µM and 43.25 µM against HCT116 and B16F10, respectively. At a concentration of 120 g/mL, the cyclopeptide Cordy A inhibited HCT116 and B16F10 cell lines with maximal % growth inhibition of 70 and 65, respectively. Cyclopeptide Cordy A demonstrated CTC50 values of 145.36 µM and 127.63 µM against HCT116 and B16F10, respectively. Lower dosages limit growth by 45 and 47.5% at 60 g/mL, respectively. The standard drug, Doxorubicin, inhibited growth by 100 percent with CTC50 values of 48.63 µM and 45.36 µM against HCT116 and B16F10, respectively. There is no inhibition in the control sample. At a 120 g/mL dosage, the cyclopeptide Oligo inhibited cell proliferation by 47.5 and 42.5 % against HCT116 and B16F10 cell lines, respectively. Cyclopeptide Oligo demonstrated CTC50 values of 175.54 µM and 139.11 µM against HCT116 and B16F10, respectively. Lower dosages decrease the growth by 35 and 32.5 percent at 60 g/mL, respectively. The conventional medication doxorubicin inhibited growth by 100 percent with CTC50 values of 48.36 µM and 46.36 µM against HCT116 and B16F10, respectively. There is no inhibition in the control sample.

The Viability assay helps figure out a number of cells that have died quantitively. It is very important for any experiment that uses cell lines or clinical samples of cells taken from outside the body. During the pre-clinical phase of drug discovery, possible drug candidates are usually tested on mammalian cell lines to see if the compound could kill cells in the body. The assay measures metabolic activity as a proxy for cell viability by reducing a yellow tetrazolium salt called 3-(4,5-dimethythiazol-2-yl)-2,5-diphenyl tetrazolium bromide, or MTT. Live cells have NAD(P)H-dependent oxidoreductase enzymes that turn the MTT reagent into formazan, an insoluble, purple-colored crystal. The more cells are alive and working their metabolism, the darker the solution.

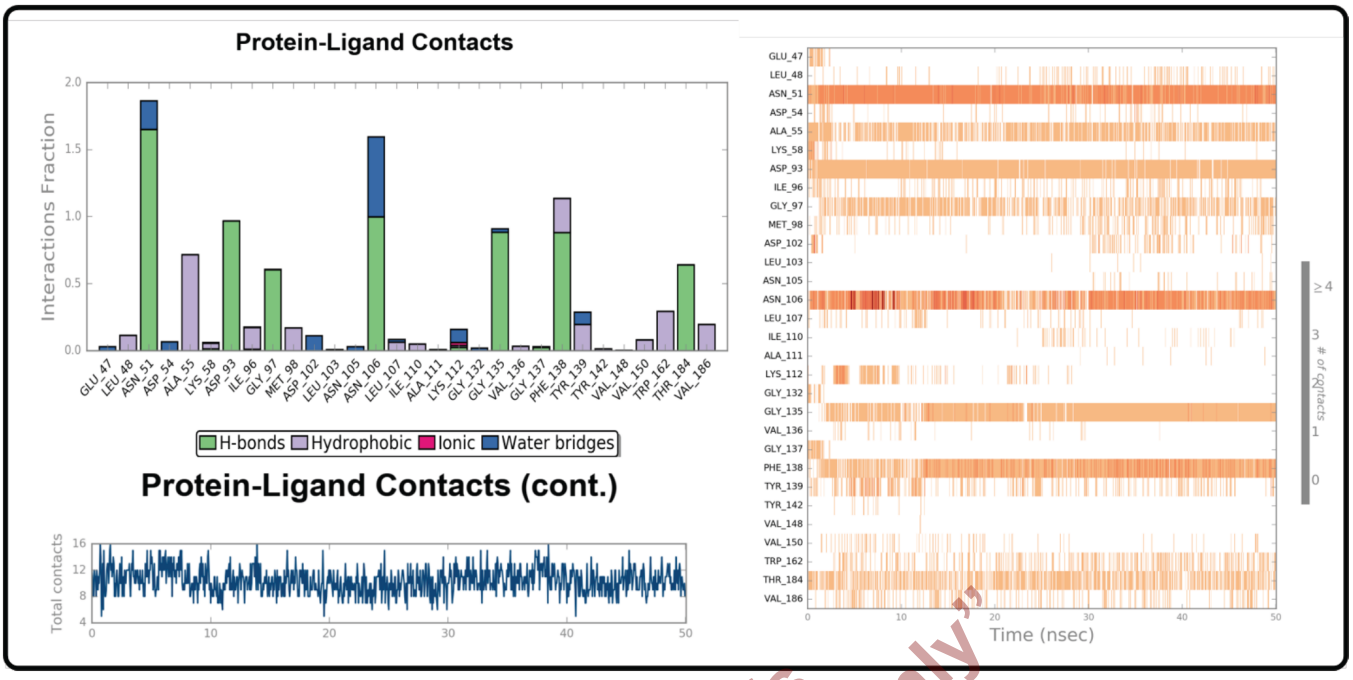

Fig. (17). Interaction fraction of various amino acid residues. (*A higher resolution / colour version of this figure is available in the electronic copy of the article*).

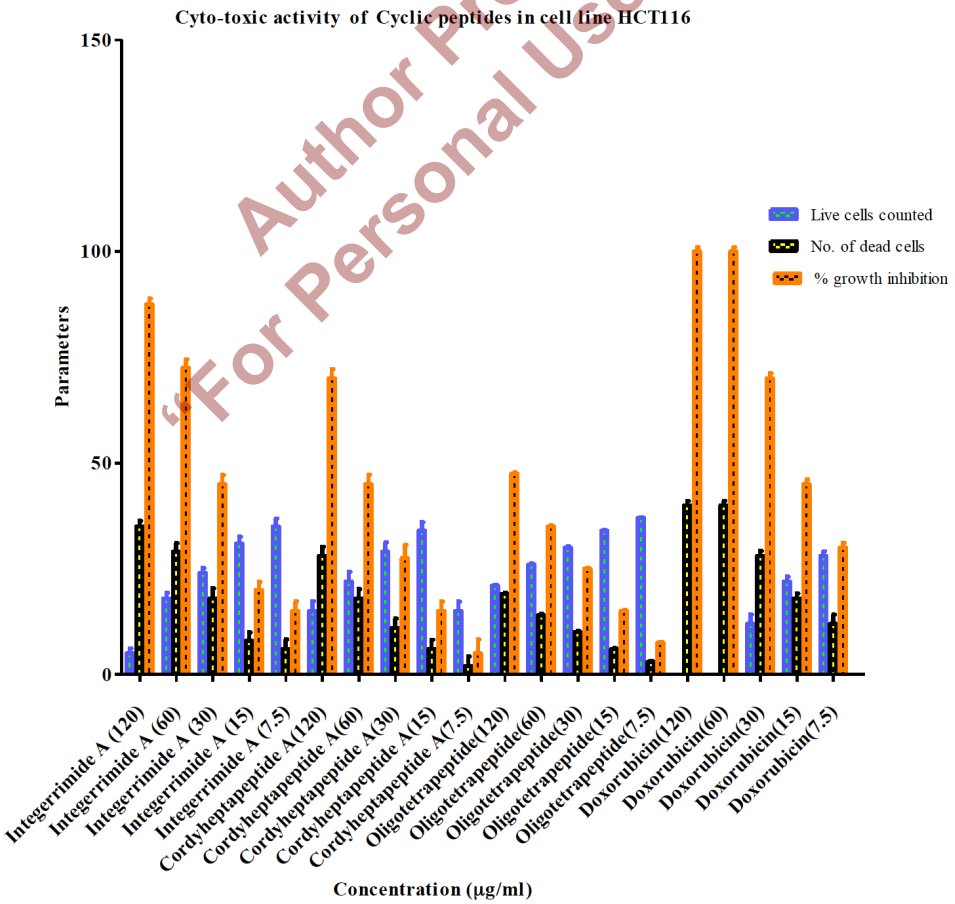

Fig. (18). Cytotoxic activity of cyclic peptides in HCT116 cell lines. All data are presented as mean ± SEM graph and are representative of three independent experiments. values **p* values < 0.05 *vs*. control, ***p* values *vs*. control ****p*<0.01, values *vs*. control *****p*<0.001, and *vs*. control. (*A higher resolution / colour version of this figure is available in the electronic copy of the article*).

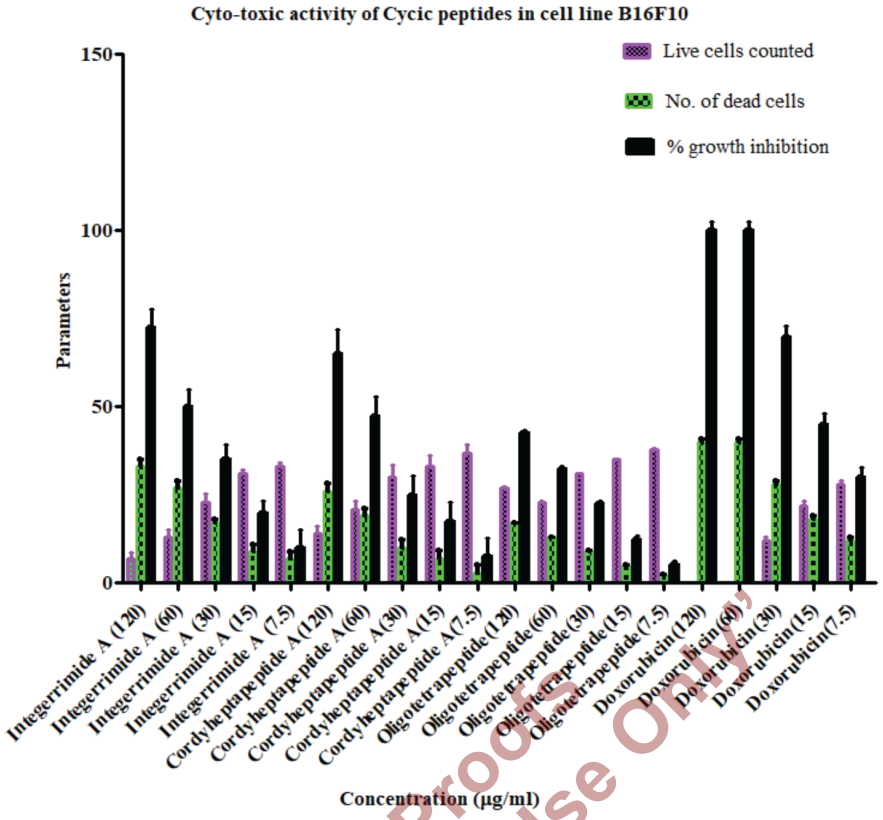

Fig. (19). Cytotoxic activity of cyclic peptides in B16F10 cell lines. All data are presented as mean ± SEM graph and are representative of three independent experiments. values **p* values < 0.05 *vs*. control, ***p* values *vs*. control ****p*<0.01, values *vs*. control *****p*<0.001, and *vs*. control. (*A higher resolution / colour version of this figure is available in the electronic copy of the article*).

Table 3. Cytotoxic effects of cyclic peptides using cell lines.

Compound	-	HCT116				B16F10			
	Concentration (µg/ml)	No. of Dead Cells	% Growth Inhibition	Counted Live Cells	$^{b}CTC_{50}$ (µM)	No. of Dead Cells	% Growth Inhibition	Counted Live Cells	$^{b}CTC_{50}$ (µM)
Int A	120	35±1.29	87.5±1.35	05±1.21	77.65	33±2.15	72.5±2.08	7±1.69	68.63
	60	29±2.01	72.5±2.03	18±1.30		27±2.15	50±1.97	13±2.14	
	30	18±2.38	45±2.14	24±1.14		17±1.02	35±1.69	23±2.31	
	15	8±1.98	20±1.88	31±1.59		9±02.11	20±1.33	31±1.05	
	7.5	06±2.34	15±2.31	35±1.87		07±2.06	10±2.04	33±1.08	
Cordy A	120	28±2.19	70±2.16	12±2.13	145.36	26±2.23	65±2.87	14±2.15	127.63
	60	18±2.21	45±2.18	22±2.25		19±2.19	47.5±2.21	21±02.24	
	30	11±2.24	27.5±3.21	29±2.27		10±2.26	25±2.23	30±3.22	
	15	6±2.22	15±2.24	34±1.98		7±2.24	17.5±2.17	33±3.23	
	7.5	02±2.25	5±3.28	38±1.94		03±2.27	7.5±2.19	37±2.21	
Oligo	120	19±0.32	47.5±0.28	21±0.23	175.54	17±0.28	42.5±0.35	27±0.25	139.11
	60	14±0.3	35±0.26	26±0.28		13±0.17	32.5±0.31	23±0.19	
	30	10±0.30	25±0.24	30±0.28		9±0.23	22.5±0.27	31±0.13	
	15	06±0.24	15±0.28	34±0.14		05±0.29	12.5±0.34	35±0.22	
	7.5	03±0.25	7.5±0.27	37±0.15		02±0.37	5.2±0.36	38±0.34	

(Table 3) contd….

Compound	-	HCT116				B16F10			
	Concentration (µg/ml)	No. of Dead Cells	% Growth Inhibition	Counted Live Cells	[b]CTC_{50} (µM)	No. of Dead Cells	% Growth Inhibition	Counted Live Cells	[b]CTC_{50} (µM)
Control (Saline)	----------	0	0	40	-	0	0	40	-
Doxorubicin (Reference)	120	40 ± 1.02	100±1.02	0	48.64	40 ± 1.02	100±1.02	0	43.27
	60	40 ± 1.02	100±1.03	0		40 ± 1.02	100±1.03	0	
	30	28 ± 1.22	70±1.21	12±1.15		28 ± 1.22	70±1.21	12±1.15	
	15	18±1.15	45±1.16	22±1.16		18±1.15	45±1.16	22±1.16	
	7.5	12±1.29	30±1.15	28±1.17		12±1.29	30±1.15	28±1.17	

$$\%\ Growth\ Inhibition^{a} = 100 - \frac{Cell_{total} - Cell_{dead}}{Cell_{total}}\ X\ 100$$

[b]CTC_{50} = Concentration Inhibiting 50% of growth

4.1. Statistical Analysis

Each experiment was repeated three times with different cell passages each time. GraphPad Prism version 8.1.0 was used for statistical analysis. The data is represented as a mean ± SEM graph. One-way analysis of variance (one-way ANOVA) was used to compare the means of treated and untreated samples, followed by a post hoc Dunnett's multiple comparison test. P-values < 0.05 were regarded as statistically significant, while $p < 0.05$, the value $p< 0.01$, values $p< 0.001$, and $p < 0.0001$ were used to indicate statistical significance.

CONCLUSION

Using an integrated approach of virtual screening, molecular docking, and dynamics simulation studies, we gained structural insights into possible binding modes of drug-like bioactive compounds against key molecular targets that play a vital role in the pathogenesis of cancer. Compound Cordy A was found to be best docked. Based on the results, almost all cyclic peptides showed cytotoxic effects on HCT116 and B16F10. The cytotoxic effects of these cyclopeptides are almost comparable to standard drug values, and these effects are found to be dose-dependent.

AUTHORS' CONTRIBUTIONS

Conceptualization A. T.; V. T. S. K. writing original draft preparation V.T. and A.T.; writing the paper and editing A. T.; V. T., S. K., M. K., S. S., R. S., N. V., B. S., D. K., R. K. S. All authors have read and approved the manuscript.

LIST OF ABBREVIATIONS

MD = Molecular Dynamics
PDB = Protein Data Bank
RMSD = Root-Mean-Square Deviation
RMSF = Root-Mean-Square Fluctuation

ETHICS APPROVAL AND CONSENT TO PARTICIPATE

Not applicable.

HUMAN AND ANIMAL RIGHTS

No animals/humans were used for studies that are the basis of this research.

CONSENT FOR PUBLICATION

Not applicable.

AVAILABILITY OF DATA AND MATERIALS

The authors confirm that the data supporting the findings of this research are available within the article.

FUNDING

None.

CONFLICT OF INTEREST

The authors declare no conflict of interest, financial or otherwise.

ACKNOWLEDGEMENTS

The authors acknowledge the Dean, Faculty of Pharmacy, IFTM University, Moradabad, for providing continuous support for the article.

REFERENCES

[1] Mathers CD, Loncar D. Projections of global mortality and burden of disease from 2002 to 2030. PLoS Med 2006; 3(11): e442. http://dx.doi.org/10.1371/journal.pmed.0030442 PMID: 17132052

[2] Lopez AD, Mathers CD, Ezzati M, Jamison DT, Murray CJL. Global and regional burden of disease and risk factors, 2001: Systematic analysis of population health data. Lancet 2006; 367(9524): 1747-57. http://dx.doi.org/10.1016/S0140-6736(06)68770-9 PMID: 16731270

[3] Bray F, Ferlay J, Soerjomataram I, Siegel RL, Torre LA, Jemal A. Global cancer statistics 2018: GLOBOCAN estimates of incidence and mortality worldwide for 36 cancers in 185 countries. CA Cancer J Clin 2018; 68(6): 394-424. http://dx.doi.org/10.3322/caac.21492 PMID: 30207593

[4] Karpuz M, Silindir-Gunay M, Ozer AY. Current and future approaches for effective cancer imaging and treatment. Cancer Biother Radiopharm 2018; 33(2): 39-51.

http://dx.doi.org/10.1089/cbr.2017.2378 PMID: 29634415
[5] Nobili S, Lippi D, Witort E, *et al.* Natural compounds for cancer treatment and prevention. Pharmacol Res 2009; 59(6): 365-78. http://dx.doi.org/10.1016/j.phrs.2009.01.017 PMID: 19429468
[6] Fridlender M, Kapulnik Y, Koltai H. Plant derived substances with anti-cancer activity: From folklore to practice. Front Plant Sci 2015; 6: 799. http://dx.doi.org/10.3389/fpls.2015.00799 PMID: 26483815
[7] Chin YW, Balunas MJ, Chai HB, Kinghorn AD. Drug discovery from natural sources. AAPS J 2006; 8(2): E239-53. http://dx.doi.org/10.1007/BF02854894 PMID: 16796374
[8] Gordaliza M. Natural products as leads to anticancer drugs. Clin Transl Oncol 2007; 9(12): 767-76. http://dx.doi.org/10.1007/s12094-007-0138-9 PMID: 18158980
[9] Loffet A. Peptides as drugs: Is there a market? J Pept Sci 2002; 8(1): 1-7. http://dx.doi.org/10.1002/psc.366 PMID: 11831558
[10] Hummel G, Reineke U, Reimer U. Translating peptides into small molecules. Mol Biosyst 2006; 2(10): 499-508. http://dx.doi.org/10.1039/b611791k PMID: 17216031
[11] Kwon YU, Kodadek T. Quantitative comparison of the relative cell permeability of cyclic and linear peptides. Chem Biol 2007; 14(6): 671-7. http://dx.doi.org/10.1016/j.chembiol.2007.05.006 PMID: 17584614
[12] Chatterjee S, Bhattacharya S, Socinski MA, Burns TF. HSP90 inhibitors in lung cancer: Promise still unfulfilled. Clin Adv Hematol Oncol 2016; 14(5): 346-56. PMID: 27379696
[13] (a) Ghaemmaghami S, Huh WK, Bower K, Howson RW. Global analysis of protein expression in yeast. Nature 2003; 425: 737-41. http://dx.doi.org/10.1038/nature02046
(b) Whitesell L, Lindquist SL. HSP90 and the chaperoning. Nature 2005; 5: 761-72. http://dx.doi.org/10.1038/nrc1716
[14] Abbasi M, Sadeghi-Aliabadi H, Amanlou M. Prediction of new Hsp90 inhibitors based on 3,4-isoxazolediamide scaffold using QSAR study, molecular docking and molecular dynamic simulation. Daru 2017; 25(1): 17. http://dx.doi.org/10.1186/s40199-017-0182-0 PMID: 28666484
[15] Sawai A, Chandarlapaty S, Greulich H, *et al.* Inhibition of Hsp90 down-regulates mutant epidermal growth factor receptor (EGFR) expression and sensitizes EGFR mutant tumors to paclitaxel. Cancer Res 2008; 68(2): 589-96. http://dx.doi.org/10.1158/0008-5472.CAN-07-1570 PMID: 18199556
[16] Goetz MP, Toft DO, Ames MM, Erlichman C. The Hsp90 chaperone complex as a novel target for cancer therapy. Ann Oncol 2003; 14(8): 1169-76. http://dx.doi.org/10.1093/annonc/mdg316 PMID: 12881371
[17] Jayaraman T, Brillantes AM, Timerman AP, *et al.* FK506 binding protein associated with the calcium release channel (ryanodine receptor). J Biol Chem 1992; 267(14): 9474-7. http://dx.doi.org/10.1016/S0021-9258(19)50114-4 PMID: 1374404
[18] Morris GM, Huey R, Lindstrom W, *et al.* AutoDock4 and AutoDockTools4: Automated docking with selective receptor flexibility. J Comput Chem 2009; 30(16): 2785-91. http://dx.doi.org/10.1002/jcc.21256 PMID: 19399780
[19] He K, Zheng X, Li M, Zhang L, Yu J. mTOR inhibitors induce apoptosis in colon cancer cells *via* CHOP-dependent DR5 induction on 4E-BP1 dephosphorylation. Oncogene 2016; 35(2): 148-57. http://dx.doi.org/10.1038/onc.2015.79 PMID: 25867072
[20] Karbowniczek M, Spittle CS, Morrison T, Wu H, Henske EP. mTOR is activated in the majority of malignant melanomas. J Invest Dermatol 2008; 128(4): 980-7. http://dx.doi.org/10.1038/sj.jid.5701074 PMID: 17914450
[21] Fukuyo Y, Hunt CR, Horikoshi N. Geldanamycin and its anticancer activities. Cancer Lett 2010; 290(1): 24-35. http://dx.doi.org/10.1016/j.canlet.2009.07.010 PMID: 19850405
[22] Van Duyne GD, Standaert RF, Schreiber SL, Clardy J. Atomic structure of the rapamycin human immunophilin FKBP-12 complex. J Am Chem Soc 1991; 113(19): 7433-4. http://dx.doi.org/10.1021/ja00019a057
[23] Ivanova L, Tammiku-Taul J, García-Sosa AT, Sidorova Y, Saarma M, Karelson M. Molecular Dynamics Simulations of the Interactions between glial cell line-derived neurotrophic factor family receptor gfrα1 and small-molecule ligands. ACS Omega 2018; 3(9): 11407-14. http://dx.doi.org/10.1021/acsomega.8b01524 PMID: 30320260
[24] Shivakumar D, Williams J, Wu Y, Damm W, Shelley J, Sherman W. Prediction of absolute solvation free energies using molecular dynamics free energy perturbation and the opls force field. J Chem Theory Comput 2010; 6(5): 1509-19. http://dx.doi.org/10.1021/ct900587b PMID: 26615687
[25] Kuttan R, Bhanumathy P, Nirmala K, George MC. Potential anticancer activity of turmeric (*Curcuma longa*). Cancer Lett 1985; 29(2): 197-202. http://dx.doi.org/10.1016/0304-3835(85)90159-4 PMID: 4075289
[26] Zou Z, Tao T, Li H, Zhu X. mTOR signaling pathway and mTOR inhibitors in cancer: Progress and challenges. Cell Biosci 2020; 10(1): 31. http://dx.doi.org/10.1186/s13578-020-00396-1 PMID: 32175074
[27] Neckers L, Workman P. Hsp90 molecular chaperone inhibitors: Are we there yet? Clin Cancer Res 2012; 18(1): 64-76. http://dx.doi.org/10.1158/1078-0432.CCR-11-1000 PMID: 22215907
[28] Stebbins CE, Russo AA, Schneider C, Rosen N, Hartl FU, Pavletich NP. Crystal structure of an Hsp90-geldanamycin complex: Targeting of a protein chaperone by an antitumor agent. Cell 1997; 89(2): 239-50. http://dx.doi.org/10.1016/S0092-8674(00)80203-2 PMID: 9108479